



**Karolinska  
Institutet**

Karolinska Institutet

<http://openarchive.ki.se>

---

This is a Peer Reviewed Accepted version of the following article, accepted for publication in Nature Cell Biology.

2019-02-11

# Reticular adhesions are a distinct class of cell-matrix adhesions that mediate attachment during mitosis

Lock, John G; Jones, Matthew C; Askari, Janet A; Gong, Xiaowei; Oddone, Anna; Olofsson, Helene; Göransson, Sara; Lakadamyali, Melike; Humphries, Martin J; Strömblad, Staffan

---

Nat Cell Biol. 2018 Nov;20(11):1290-1302.

<http://doi.org/10.1038/s41556-018-0220-2>

<http://hdl.handle.net/10616/46640>

*If not otherwise stated by the Publisher's Terms and conditions, the manuscript is deposited under the terms of the Creative Commons Attribution-NonCommercial-NoDerivatives License (<http://creativecommons.org/licenses/by-nc-nd/4.0/>), which permits non-commercial re-use, distribution, and reproduction in any medium, provided the original work is properly cited, and is not altered, transformed, or built upon in any way.*



**Karolinska  
Institutet**

This is a post-peer-review, pre-copyedit version of an article published in Nature Cell Biology.

The final authenticated version is available online at:  
**<http://dx.doi.org/10.1038/s41556-018-0220-2>**

This paper has been peer-reviewed but does not include the final publisher proof-corrections or journal pagination.

Citation for the published paper:

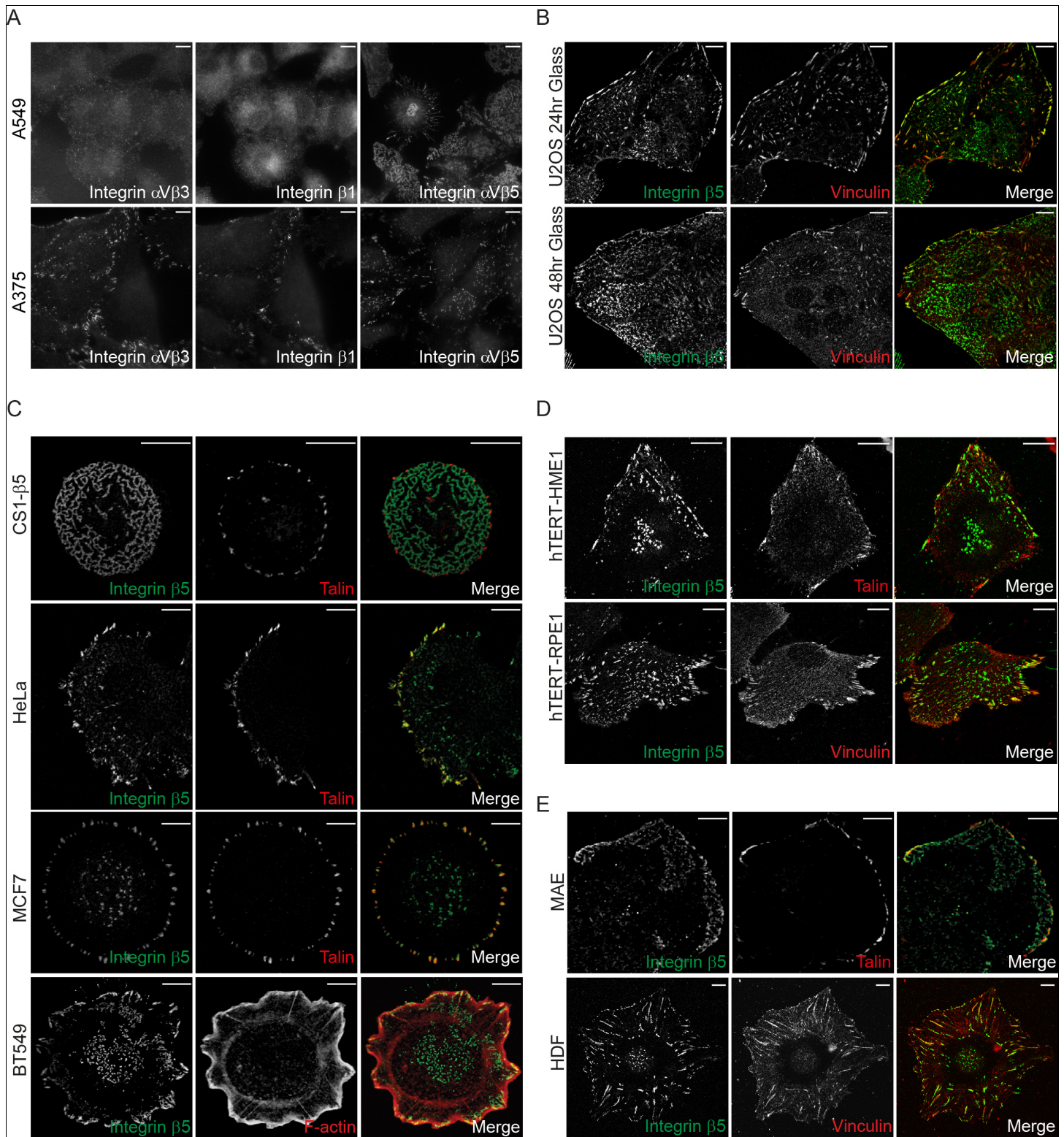
Lock JG, Jones MC, Askari JA, Gong X, Oddone A, Olofsson H, Göransson S, Lakadamyali M, Humphries MJ, Strömblad S.

Reticular adhesions are a distinct class of cell-matrix adhesions that mediate attachment during mitosis.

Nat Cell Biol. 2018 Nov;20(11):1290-1302

Access to the published version may  
require subscription.

Published with permission from: **Springer Nature**



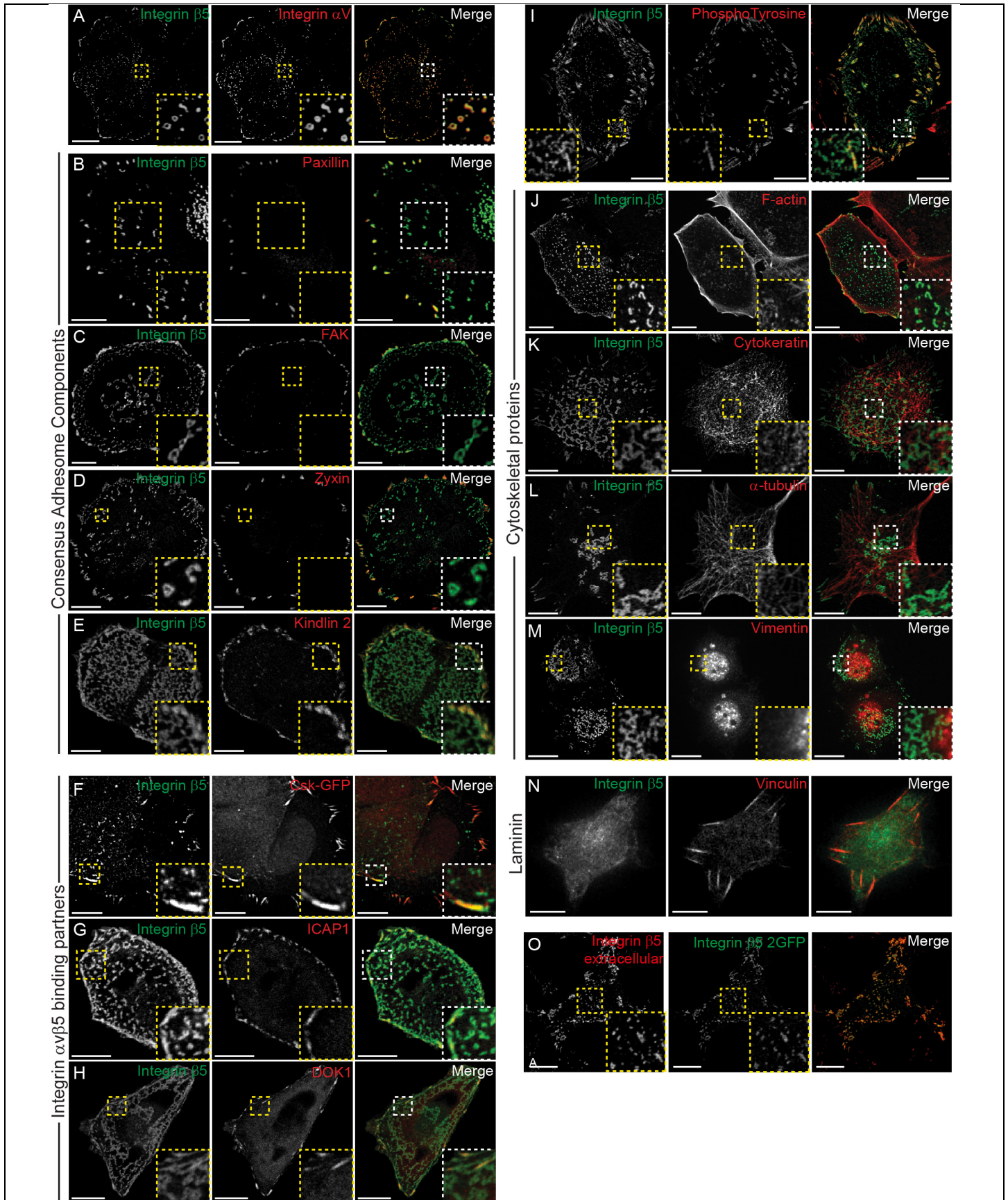
**Supplementary Figure 1**

***$\beta 5$ -positive, talin- or F-actin-negative structures found in multiple cell lines.***

(A) A549 lung cancer cells and A375 melanoma cells plated on glass coverslips for 72 h. Confocal images of

immuno-fluorescently labeled integrins  $\alpha$ V $\beta$ 3 (LM609),  $\beta$ 1 (9EG7) and  $\alpha$ V $\beta$ 5 (15F11). (B) U2OS cells plated on glass coverslips for 24 and 48 h. Confocal images of immuno-fluorescently labeled integrin  $\beta$ 5 and vinculin. (C,D,E) The indicated human-, mouse- and hamster-derived cancer cell lines (C), immortalized diploid cell lines (D) and primary cells (E) were found to contain central  $\beta$ 5-positive, talin- and F-actin-negative structures equivalent to those first observed in U2OS cells. Confocal images of cells replated for 3 h on 10  $\mu$ g/ml vitronectin and immuno-labeled for integrin  $\beta$ 5 and either talin or F-actin, as indicated. All images representative of results from at least n = 3 biologically independent experiments. Scale bars: 10  $\mu$ m.

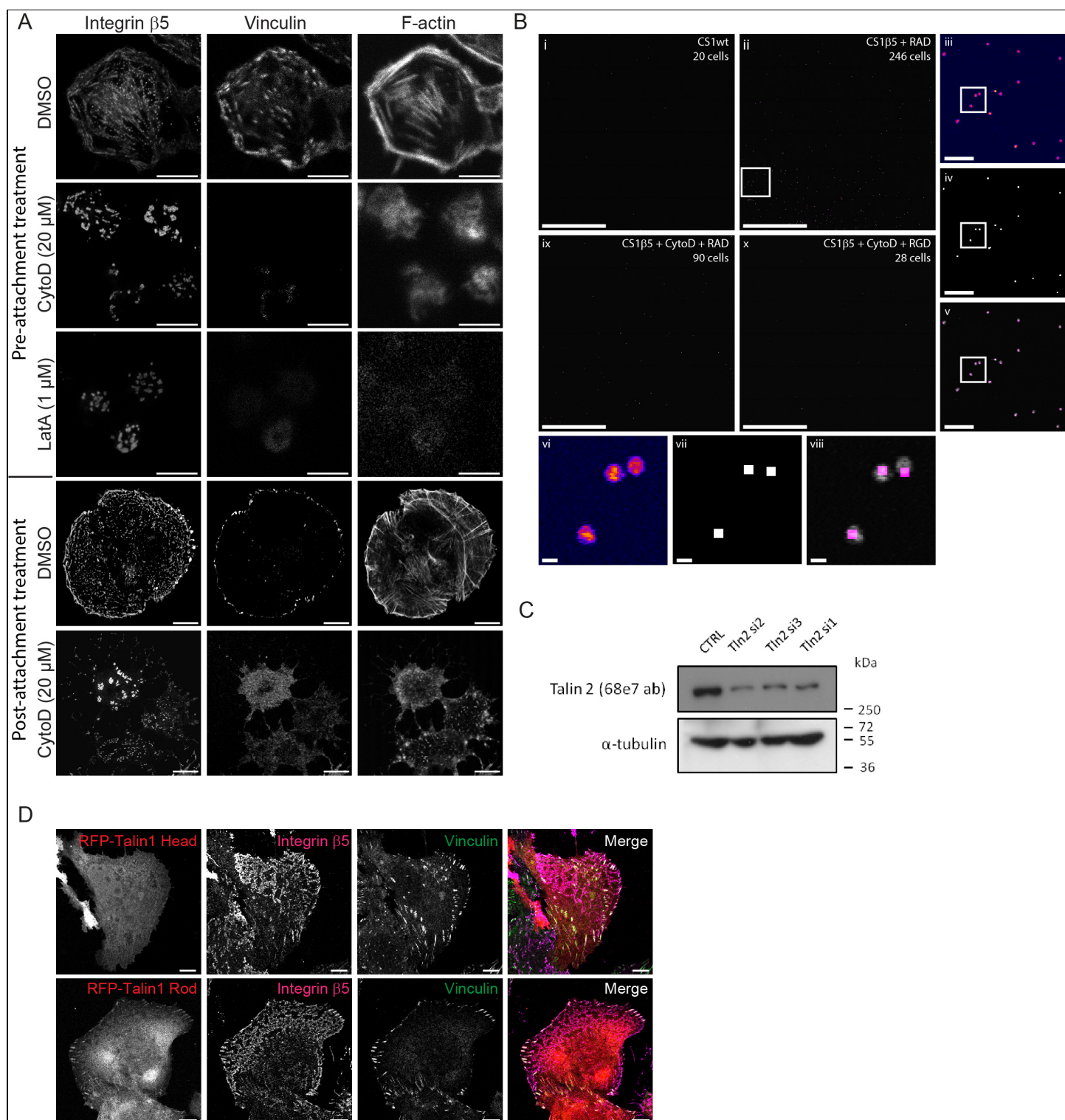




## Supplementary Figure 2

### *$\beta$ 5-positive reticular adhesions lack consensus adhesome components*

(A-M) Confocal images of U2OS cells plated for 3 h on vitronectin and immuno-labeled against integrin  $\beta$ 5 and: the alpha V ( $\alpha$ V) subunit of the  $\alpha$ V $\beta$ 5 heterodimer (A); consensus adhesome components [paxilin (B), FAK (C), zyxin (D), kindlin 2 (E)]; integrin  $\beta$ 5-binding partners [CSK (genetically encoded GFP-CSK) (F), ICAP1 (G), DOK1 (H)]; phospho-tyrosine (I); and cytoskeletal proteins [F-actin (J), cytokeratin (K), beta ( $\beta$ )-tubulin (L), vimentin (M)]. (N) Confocal image of U2OS cells plated for 3 h on laminin (ECM ligand not bound by  $\alpha$ V $\beta$ 5) and immuno-labeled for integrin  $\beta$ 5 and vinculin. (O) Confocal images of an unpermeabilised U2OS cell expressing  $\beta$ 5-2GFP, immuno-labeled for  $\beta$ 5. All images representative of results from at least n = 3 biologically independent experiments. Scale bars: 10  $\mu$ m. Boxed areas shown at higher magnification in lower right corners.



**Supplementary Figure 3**

***Validation of reticular adhesion independence from F-actin and talin***

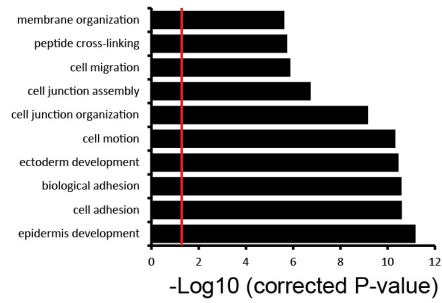
(A, upper) Confocal images of U2OS cells attached to vitronectin (VN)-coated surfaces and labeled for integrin  $\beta 5$ , vinculin and F-actin, following 30 min in suspension and 3 h replating in presence of DMSO, 20  $\mu$ M

cytochalasin D (CytoD), or 1  $\mu$ M latrunculin A (LatA). (A, lower) Representative confocal images of U2OS cells attached to vitronectin (VN)-coated surfaces and labeled for integrin  $\beta$ 5, vinculin and F-actin, following 3 h replating, with final 1 h in presence of DMSO or 20  $\mu$ M CytoD. (B) Images comparing attachment of CS1WT or CS1 $\beta$ 5 cells to vitronectin in the presence of RAD or RGD peptides and/or CytoD. Zoomed panels demonstrate image-based identification of attached cells using automated cell counting in NIS Elements. Representative of n = 6 biologically independent experiments. (C) Representative immunoblot of talin 2 (68e7 antibody) and tubulin following siRNA treatment with control (CTRL) oligonucleotides or one of three alternative talin 2-targeting oligonucleotides. Unprocessed blots in Supplementary Fig 9. (D) Confocal images of U2OS cells expressing RFP-talin head or RFP-talin rod domains plated on glass coverslips for 48 hours and immunolabeled for integrin  $\beta$ 5 and vinculin. Images in A, C-D representative of results from at least n = 3 biologically independent experiments. Scale bars: A, B<sub>vi-viii</sub> = 10  $\mu$ m; B<sub>i-ii</sub> and B<sub>ix-x</sub> = 1000  $\mu$ m; B<sub>iii-v</sub> = 100  $\mu$ m; D = 5  $\mu$ m.



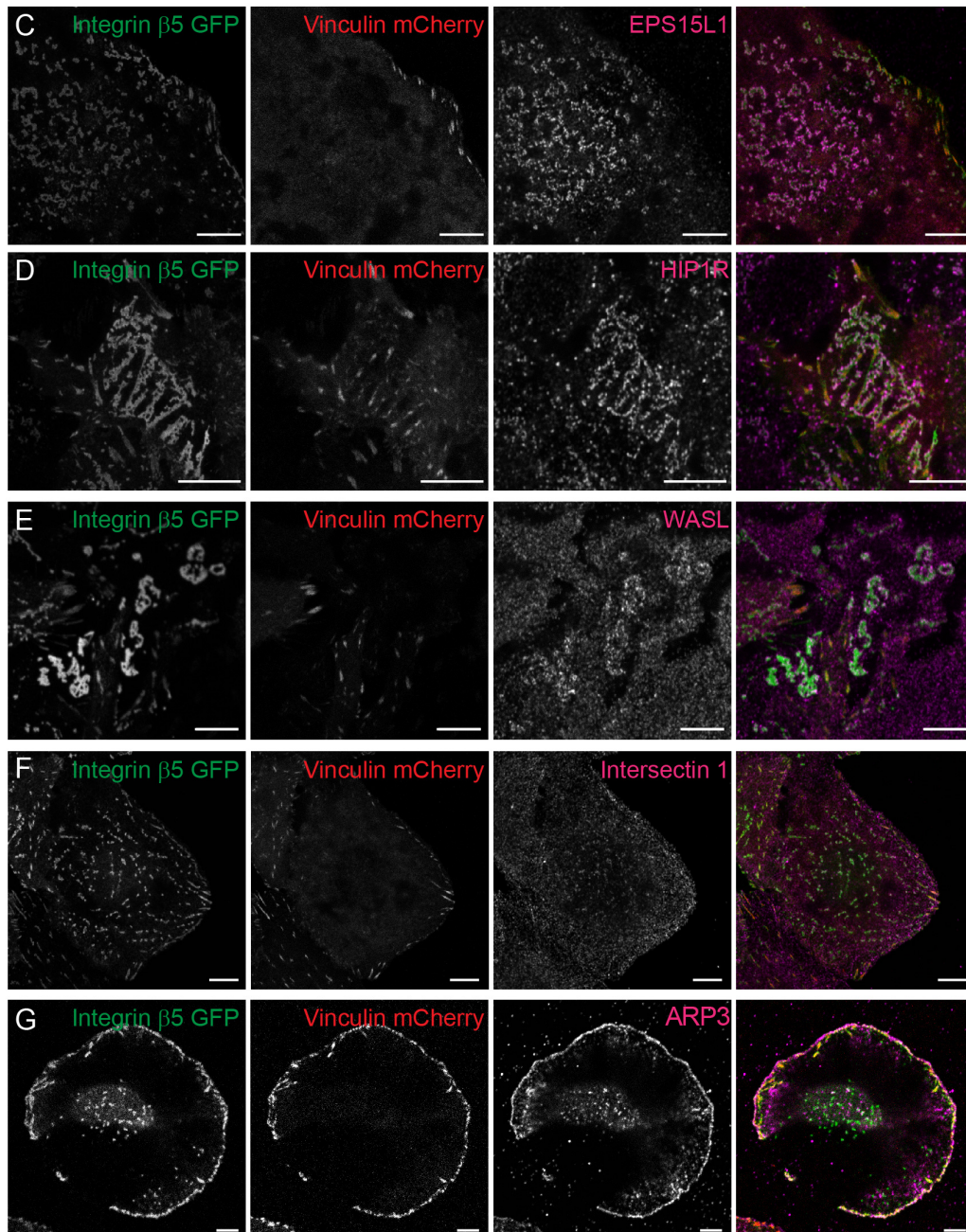
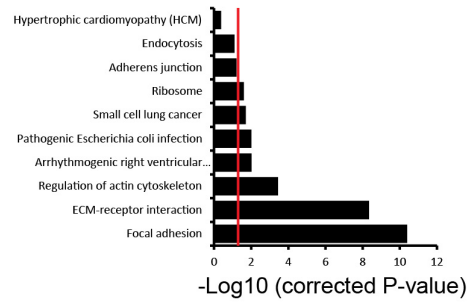
A

## U2OS Steady State Adhesions: Biological Process



B

## U2OS Steady State Adhesions: KEGG Pathway

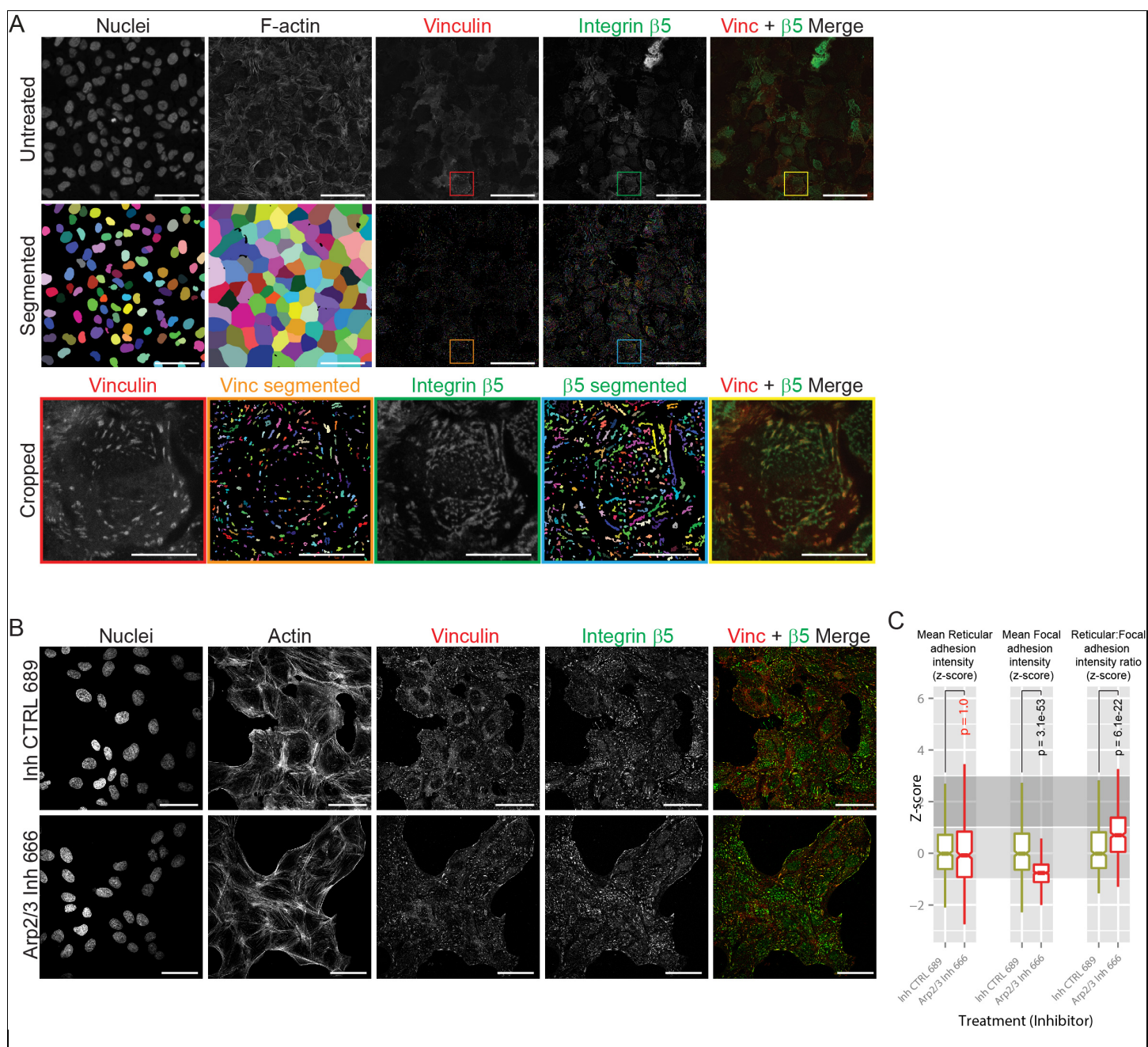




#### Supplementary Figure 4

##### *Validation of reticular adhesion proteins identified by mass spectrometry*

(A,B) Gene-ontology analysis of U2OS steady state adhesion proteins (DMSO treated; focal and reticular adhesions) showing terms from Biological Process (A) and KEGG pathway analysis (B) significantly enriched over whole cell proteome (based on data from n = 3 biologically independent mass spec experiments). P-values were derived from EASE scores calculated using a modified Fishers Exact test with Holm-Bonferroni correction from multiple tests using the DAVID annotation system. (C-G) Confocal images of U2OS  $\beta$ 5V cells attached to vitronectin (VN)-coated surfaces and immuno-labeled against EPS15L1 (C), HIP1R (D), or WASL (E), Intersectin-1 (F), and ARP3 (G). All images representative of results from at least n = 3 biologically independent experiments. Scale bars: C-E = 10  $\mu$ m; F-G = 5  $\mu$ m.

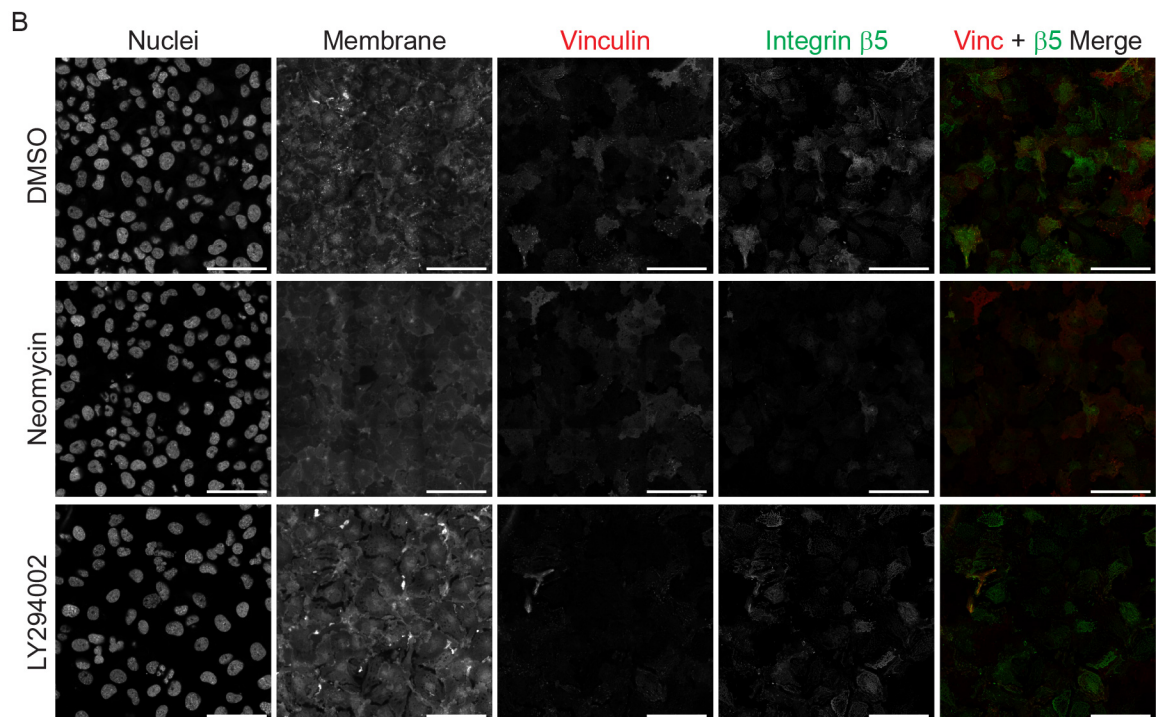
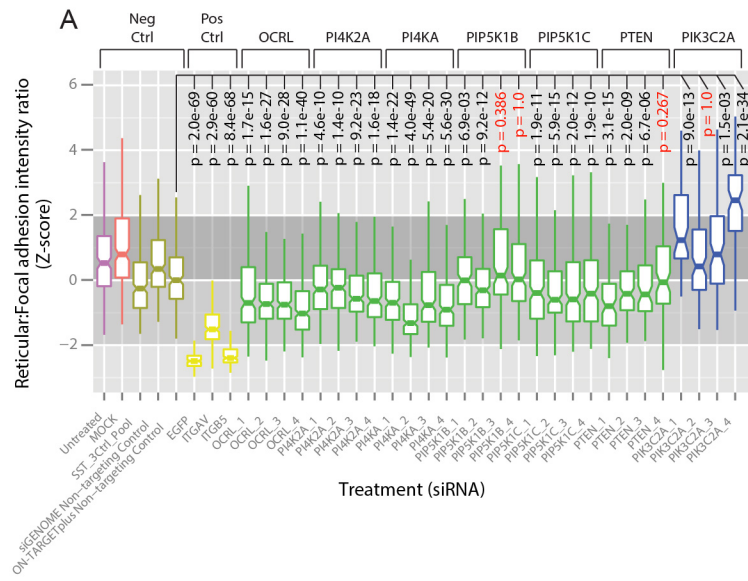


**Supplementary Figure 5**

### **Quantitative imaging of siRNA- or Arp2/3 inhibitor-treated cells**

(A) Representative images illustrating segmentation of U2OS cells based on DAPI (nuclei) and F-actin staining and subsequent segmentation of mCherry-vinculin and integrin  $\beta 5$ -2GFP fluorescence (shown for an individual cell; cropped). Images representative of  $n = 2$  biologically independent experiments. Scale bars 50  $\mu\text{m}$  (10  $\mu\text{m}$  in cropped images). (B) Representative images of U2OS cells stained with DAPI (nuclei) and phalloidin, and immunolabelled for integrin  $\beta 5$  and vinculin following treatment with Arp2/3 inhibitor (CK-666) or inactive analogue control (CK-689). Scale bars = 50  $\mu\text{m}$ . (C) Boxplots summarizing single cell quantification (from images as shown in B;  $n = 1019$  cells analysed, averaging 509  $\pm$  23 (stdev) per condition) of reticular to focal

adhesion integrin  $\beta 5$  ratios following treatment with Arp2/3 inhibitor (CK-666) or inactive analogue control (CK-689). Boxplot centre and box edges indicate median and 25<sup>th</sup> or 75<sup>th</sup> percentiles, respectively, while whiskers indicate the median  $\pm$  1.5\*IQR (inter-quartile range) or the most extreme observations within these limits. Boxplot notches approximate 95% confidence intervals (CI; see methods for details). P-values reflect two-sided unpaired Mann Whitney U testing. Images and data in B-C derived from 3 biologically independent experiments. Source data for C is available in Supplementary Table 1.



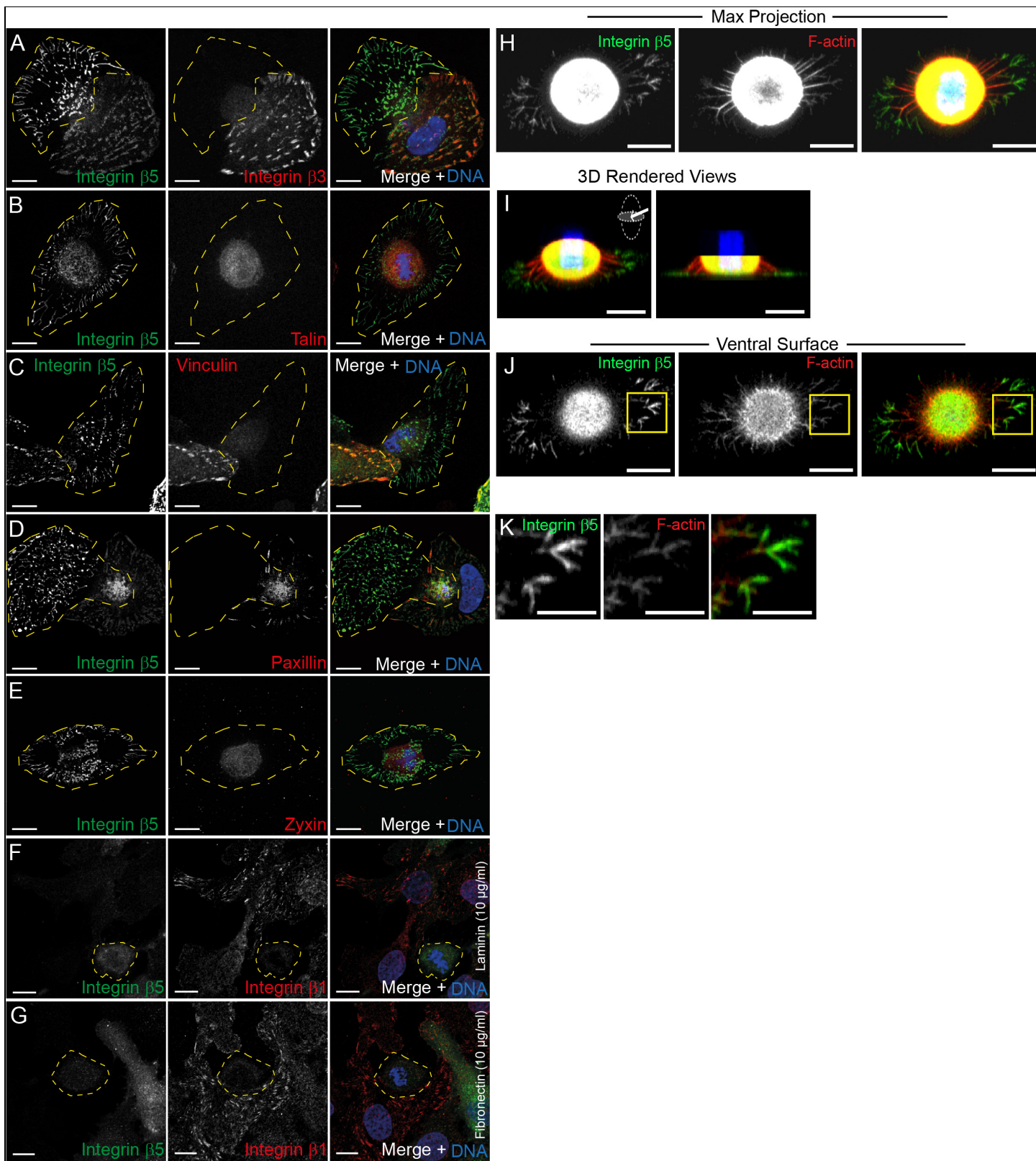
**Supplementary Figure 6**

### ***Secondary siRNA validation and effects of PI4,5P2 modulation***

(A) Single cell quantification (n = 8070 cells analysed, averaging 224 +/- 63 (stdev) per condition) of reticular to focal adhesion integrin  $\beta 5$  ratios for 4 independent siRNAs targeting controls or PIP regulators. Boxplot centre and box edges indicate median and 25<sup>th</sup> or 75<sup>th</sup> percentiles, respectively, while whiskers indicate the median +/- 1.5\*IQR (inter-quartile range) or the most extreme observations within these limits. Boxplot notches approximate 95% confidence intervals (see methods for details). P-values reflect two-sided unpaired Mann

Whitney U testing with Holm-Bonferroni correction from multiple tests. Data derived from 2 biologically independent experiments. Source data is available in Supplementary Table 1 (B) Representative images of U2OS cells stained with DAPI (nuclei) and deep red cell mask membrane dye and showing integrin  $\beta$ 5-2GFP and mCherry-vinculin fluorescence following treatment with DMSO, 10 mM Neomycin or 25  $\mu$ M LY294002. Images in B representative of n = 3 biologically independent experiments. Scale bars = 50  $\mu$ m.

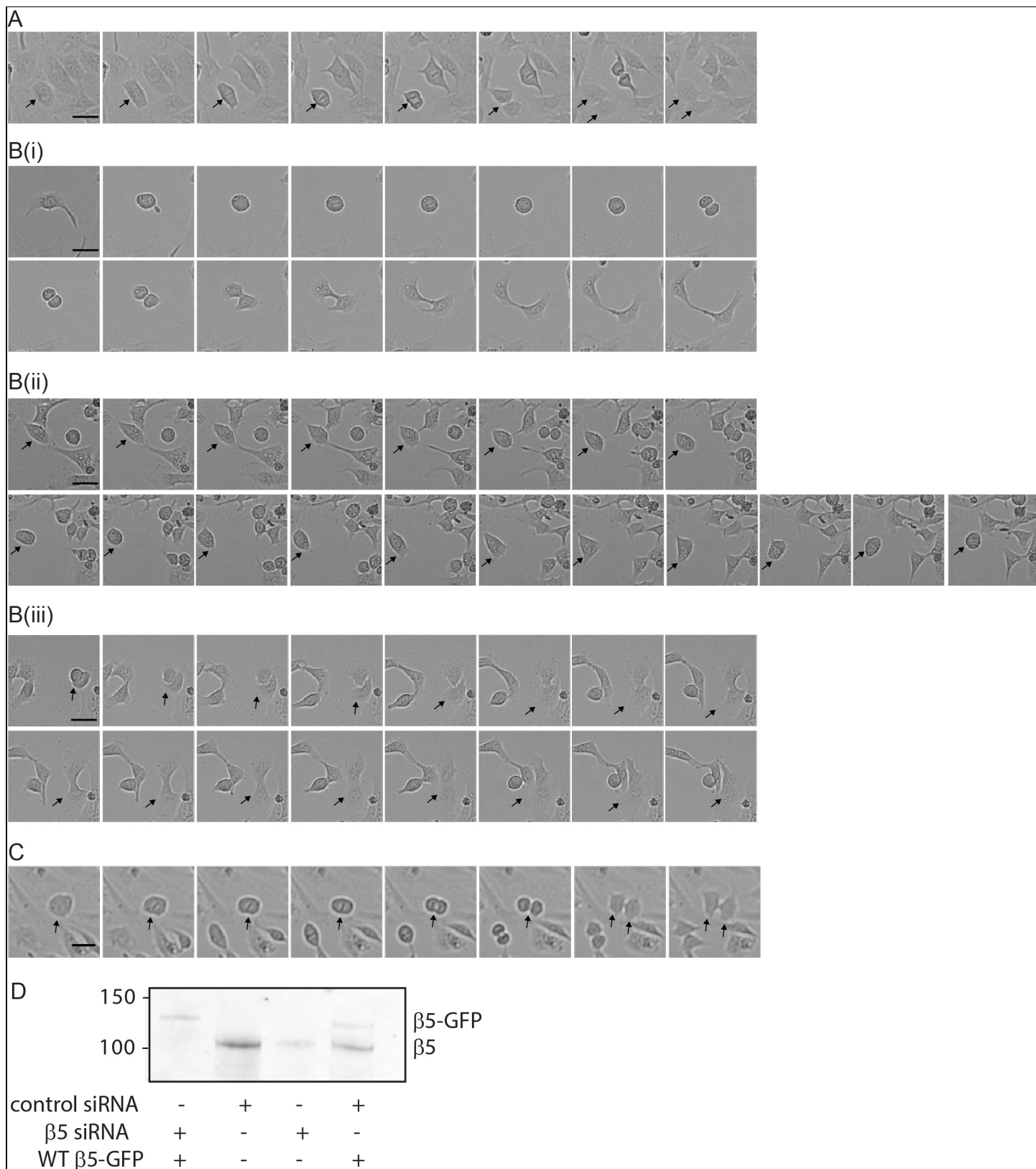




Supplementary Figure 7

### ***Mitotic reticular adhesions lack canonical adhesome components***

(A-E) Confocal images of mitotic U2OS cells (yellow dashed outlines) plated on VN and labeled for integrin  $\beta 5$  and: integrin  $\beta 3$  subunit (A); and consensus adhesome components [talin (B), vinculin (C), paxillin (D), zyxin (E)]. (F-G) Confocal images of mitotic U2OS cells plated on 10 $\mu$ g/ml laminin (F) or fibronectin (G) immunolabeled against integrin  $\beta 5$  and integrin  $\beta 1$  subunits. Images in A-K representative of at least  $n = 3$  biologically independent experiments. (H-K) Alternate views of actin-positive retraction filaments (phalloidin-labeled) formed during mitosis and terminating at integrin  $\beta 5$ -2GFP-positive adhesion complexes (K cropped from yellow box in J; see **Supplementary Movie 9**). Images in H-K representative of  $n = 2$  biologically independent experiments. Scale bars: 10  $\mu$ m except in K; 5  $\mu$ m.

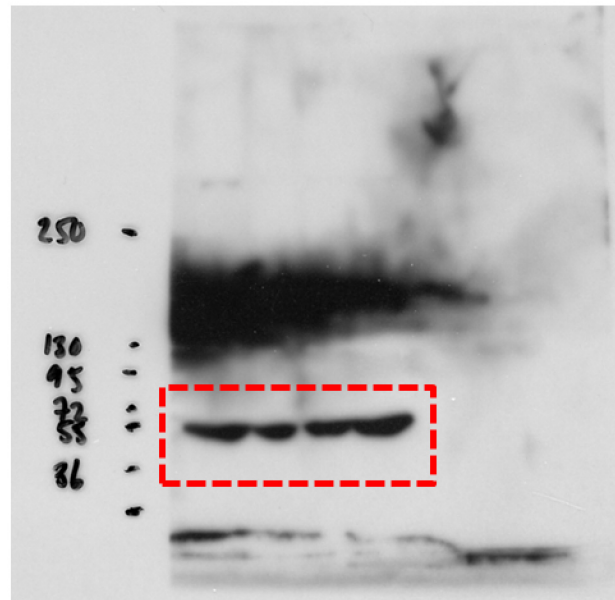
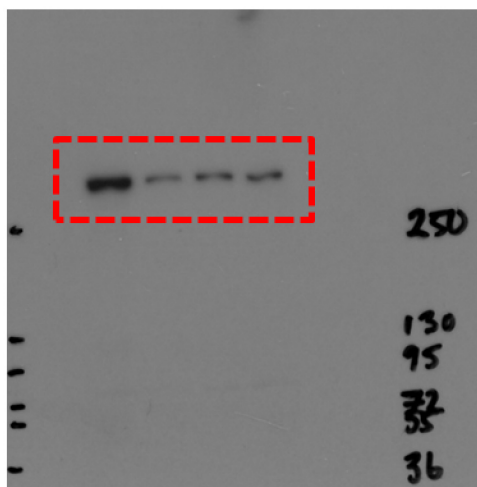


**Supplementary Figure 8**

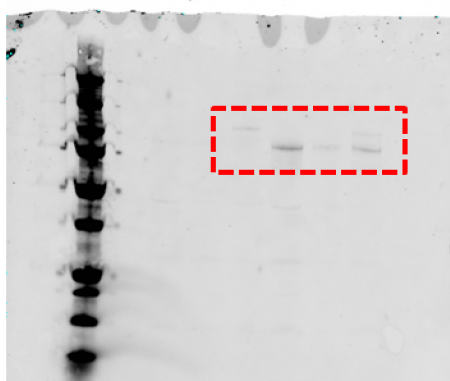
### ***Disruption of HeLa cell mitosis by integrin $\beta 5$ siRNA***

(A) HeLa cells transfected with control siRNA showing normal cell division (see **Supplementary Movie 10**). (B) Three example microscopy time series representative of different effects of depleting  $\beta 5$  on cell division: i) cell remains round for an extended time before eventually dividing, often with incomplete cytokinesis (see **Supplementary Movie 11**). ii) cell repeatedly rounds up and respreads without dividing (see **Supplementary Movie 12**). iii) cell appears to divide but before cytokinesis merges back into a single bi-nucleate cell (see **Supplementary Movie 13**). (C) HeLa cell treated with  $\beta 5$  siRNA and rescued with  $\beta 5$ -EGFP (see **Supplementary Movie 14**). (A-C) Images were taken at 10 min intervals. Arrows point to mitotic cells of interest. Images representative of  $n = 3$  biologically independent experiments. (D) Representative immunoblot of endogenous and  $\beta 5$ -EGFP expression in control and knockdown cells. Unprocessed blot in Supplementary Fig 9. Scale bars = 50  $\mu\text{m}$ .

A



B



Supplementary Figure 9

*Unprocessed images of all gels and blots*

(A) Unprocessed blots from figure SF3C. Film from talin2 blot was accidentally cut at the bottom because the background was too low to see where the membrane ended. (B) Unprocessed blot from figure SF8D.



### ***Supplementary Table 1. Statistics Source Data***

This excel file contains all quantitative data underpinning this study. Data pertaining to each graphical figure panel is arranged in separate sheets. In some cases, plots are generated directly within Excel, however in the majority of cases, data is called for further statistical analysis and plot generation using the R markdown file “Statistical\_Analysis\_Code\_Lock\_et\_al\_NCB\_2018.Rmd” which can be accessed via the GitHub repository associated with this study.

### ***Supplementary Table 2. Proteomic characterisation of reticular adhesions***

This table provides raw abundance values of proteins identified by mass-spectrometry following treatment with either DMSO or cytochalasin D for 3 independent experiments. The combined fold-change data used to calculate the mean fold change in protein abundance following treatment with cytochalasin is also presented along with the list of proteins that constitute the reticular adhesome.

### ***Supplementary Table 3. Direct and indirect PI45P2 interactors***

This table provides references to evidence of direct or indirect interactions between reticular adhesome components and PI(4,5)P2. Indirect interactors are limited in this case to ‘1 hop’ interactions, meaning interaction through a single binding partner intermediary.

### ***Supplementary Table 4. Details of antibodies used***

This table contains information on the antibodies used in this study, including their: targets, applied concentrations, validation and sources.

### ***Supplementary Table 5. PIP regulator siRNA screen oligonucleotide sequences***

This table provides sequences for each of the siRNA oligonucleotide sequences used in the PIP regulator screen.

### ***Supplementary Movie 1. Reticular adhesion formation, maturation and turnover***

Confocal live cell imaging of U2OS  $\beta$ 5V cells at 10 min intervals for 12 h, as depicted in Figure 2E-G. mCherry-vinculin (left, red in merge), integrin  $\beta$ 5-2GFP (centre, green in merge) and merge (right) channels demarcate reticular (mCherry-vinculin-negative; typically more centrally located) and classical focal adhesions (mCherry-vinculin-positive; typically peripherally located). Note that reticular adhesions form, mature and disassemble without ever showing mCherry-vinculin concentration. Representative example of  $n = 4$  biologically independent experiments.

### ***Supplementary Movie 2. Reticular adhesions do not recruit vinculin during their lifetime***

Confocal live cell imaging of U2OS- $\beta$ 5V cells at 10 min intervals for 12 h, cropped from Supplementary Movie 1 (as indicated in Figure 2E-G), as depicted in Figure 2H. mCherry-vinculin (left, red in merge), integrin  $\beta$ 5-2GFP (centre, green in merge) and merge (right) channels. Integrin  $\beta$ 5 2GFP demarcates the formation, maturation and disassembly of a single reticular adhesion. Note that this complete life cycle occurs without the recruitment of any detectable concentration of mCherry-vinculin. Representative example of  $n = 4$  biologically independent experiments.

### ***Supplementary Movie 3. Comparison of reticular and focal adhesion dynamics***

Spinning-disc confocal live cell imaging of U2OS- $\beta$ 5V cells at 10 min intervals for 12.5 h, as depicted in Figure 2I-M. (Upper panels) mCherry-vinculin (left, red in merge), integrin  $\beta$ 5 2GFP (centre, green in merge) and merge (right) channels. (Low panels) Focal adhesion tracking demarcated by mCherry-vinculin (left, tracks rainbow colour-coded indicating recent (blue-to-green) and old (orange-to-red) movements), focal adhesion and reticular adhesion tracking demarcated by integrin  $\beta$ 5-2GFP (centre, tracks rainbow colour-coded indicating recent (blue-to-green) and old (orange-to-red) movements) and merged tracking results (right) channels. Note that the subset of reticular adhesion dynamics was specifically extracted for quantitative analyses by parsing tracking results with quantification of mCherry-vinculin content (intensity) in integrin  $\beta$ 5-2GFP-defined adhesions, using the criteria described in methods. Representative example of  $n = 4$  biologically independent experiments.

### ***Supplementary Movie 4. FRAP comparison of integrin $\beta$ 5 2GFP***

Confocal-based fluorescence recovery after photobleaching (FRAP) analysis of U2OS- $\beta$ 5V cells to compare integrin  $\beta$ 5-2GFP turnover rates in reticular versus focal adhesions, as depicted in Figure 2O-T and described in methods. mCherry-vinculin (left, red in merge), integrin  $\beta$ 5-2GFP (centre, green in merge) and merge (right). Representative example of  $n = 3$  biologically independent experiments.

### ***Supplementary Movie 5. Reticular adhesion formation during cell-ECM attachment in the presence and absence of F-actin***

Confocal images of integrin  $\beta$ 5-2GFP and mCherry-vinculin in live U2OS- $\beta$ 5V cells over 3.6 h post attachment to vitronectin-coated glass, as detailed in Figure 3. Cells were pre-treated in suspension (30 min) and during spreading with either DMSO (upper panels) or 20  $\mu$ M of F-actin polymerization inhibitor

cytochalasin D (CytoD; lower panels). Integrin  $\beta 5$ -2GFP (left, green in merge), mCherry-vinculin (centre, red in merge) and merge (right) channels. Representative example of  $n = 3$  biologically independent experiments.

***Supplementary Movie 6. Reticular adhesions persist throughout cell division when classical focal adhesions disassemble***

Spinning-disc confocal live cell imaging of U2OS- $\beta 5$ V cells at 10 min intervals for 16.5 h, as depicted in Figure 6C-I. (Upper panels) Membrane dye (left, magenta in merge), mCherry-vinculin (centre left, red in merge), integrin  $\beta 5$ -2GFP (centre right, green in merge) and merge (right) channels. (Lower panels) Intensity color-coded ('fire' look-up table scales from low intensity to high via black, red, yellow, white) mCherry-vinculin signal (left), and segmented and tracked vinculin-labeled focal adhesions (centre left; red outlines) and cell outline (blue outline demarcated by membrane dye). Note loss of focal adhesions during mitosis. Intensity color-coded ('fire look-up table) integrin  $\beta 5$ -2GFP (centre right) and segmented and tracked reticular and focal adhesions (right; red outlines) as well as cell outline (blue outline). Representative example of  $n = 5$  biologically independent experiments.

***Supplementary Movie 7. Mitotic retraction fibres attach to ECM at reticular adhesion sites***

3-dimensional confocal reconstruction of a U2OS- $\beta 5$ V cell mid-mitosis, as depicted in Figure 6J-L. Membrane labelling (red) demarcates the cell body and retraction fibres angling down from the cell cortex to the ECM interface. Retraction fibres terminate in integrin  $\beta 5$  2GFP-decorated reticular adhesions (green). DNA is revealed in compacted form (white) via a progressive cut-through of the reconstructed view from the dorsal surface. Representative example of  $n = 5$  biologically independent experiments.

***Supplementary Movie 8. Post-mitotic daughter cells re-spread via retraction fibres tethered to the ECM by reticular adhesions, thereby recovering the pre-mitotic footprint***

4-dimensional confocal reconstruction of a U2OS- $\beta 5$ V cell imaged at 10 min intervals during the re-spreading of daughter cells post-mitosis. Membrane labelling (red) demarcates the cell body and retraction fibres angling down from the cell cortex to the ECM interface. Retraction fibres terminate in integrin  $\beta 5$ -2GFP-decorated reticular adhesions (green). DNA (blue) revealed via a cut-through of the reconstructed view. Representative example of  $n = 5$  biologically independent experiments.

***Supplementary Movie 9. Mitotic retraction fibres contain dense F-actin labeling while reticular adhesion sites have only weak F-actin labeling***

3-dimensional confocal reconstruction of a U2OS cell mid-mitosis, as depicted in Figure 6O-R. F-actin is labeled with phalloidin (red), while  $\beta 5$ -2GFP demarcates mitotic reticular adhesions. F-actin is concentrated in retraction fibres that angle down from the cell cortex to the ECM interface, terminating in integrin  $\beta 5$ -2GFP-decorated reticular adhesions. Only weak F-actin labeling colocalizes with mitotic reticular adhesions. DNA is revealed in compacted form (DAPI; blue) via a progressive cut-through of the

reconstructed view from the dorsal surface. Representative example of  $n = 2$  biologically independent experiments.

***Supplementary Movie 10. Individual centrally located reticular adhesions persist throughout mitosis***

Spinning-disc confocal live cell imaging of U2OS- $\beta 5$ V cells at 10 min intervals for 13 h 50 min. Integrin  $\beta 5$ -2GFP (left, green in merge), mCherry-vinculin (centre, red in merge) and merge (right) channels. Note the persistence of integrin  $\beta 5$  2GFP-decorated reticular adhesions throughout mitosis when classical focal adhesions labeled by mCherry-vinculin disassemble. In particular, note that centrally located reticular adhesions are morphologically stable throughout mitosis, indicating that the same individual reticular adhesions persist throughout mitosis, not only the reticular adhesion population in general. This supports a role for reticular adhesion in retention of spatial memory from one cell generation the next. Representative example of  $n = 5$  biologically independent experiments.

***Supplementary Movie 11. Cell division in HeLa cells after synchronisation***

HeLa cells, transfected with control siRNA, were synchronised by double thymidine block and imaged 8 h after second release. Images were taken every 10 min for a further 320 min. Movie shows normal cell division taking approximately 70 min to complete. Representative example of  $n = 3$  biologically independent experiments.

***Supplementary Movies 12-14. Defects in cell division after integrin  $\beta 5$  knockdown***

HeLa cells transfected with integrin  $\beta 5$  siRNA were synchronised and imaged as above, related to Fig 8C. Movies show different mitotic defects that resulted. **Movie 12** cell remained rounded for an extended period of time often with incomplete cytokinesis. **Movie 13** cell repeatedly rounds up and respreads without dividing. **Movie 14** cell appeared to divide but before cytokinesis merged to form a bi-nucleate cell. Representative example of  $n = 3$  biologically independent experiments.

***Supplementary Movie 15. Rescue of cell division defects by wild type integrin  $\beta 5$***

HeLa cells transfected with integrin  $\beta 5$  siRNA together with WT  $\beta 5$ -EGFP were synchronised and imaged as above, related to Fig 8C. Movie shows rescue of mitotic defects. Representative example of  $n = 3$  biologically independent experiments.